MULTICRITERIA ANALYSIS OF IMPACTS OF DISTRIBUTED GENERATION SOURCES ON OPERATIONAL NETWORK CHARACTERISTICS FOR DISTRIBUTION SYSTEM PLANNING CONCERNING STEADY-STATE AND TRANSIENT OPERATIONS

Alexandre Barin[1], Luis F. Pozzatti[1], Ricardo Q. Machado[2], Luciane N. Canha[1], Felix A. Farret[1], Alzenira da R. Abaide[1]

[1]Federal University of Santa Maria, Brazil
CEEMA/UFSM - Avenida Roraima,1000, Bairro Camobi – Santa Maria – RS – Brasil – CEP: 97105-900
Phone: +55 55 32208792
E-mail: alexandrebarin@hotmail.com; fila_rs@hotmail.com; lncanha@ufsm.ct.br; faf@ct.ufsm.br , alzenira@ct.ufsm.br

[2]University of São Paulo, Brazil
EESC/USP - Avenida Trabalhador São-Carlense, 400 – São Carlos – SP – Brasil – CEP: 13566-590
Phone: +55 16 33738277
E-mail: rquadros@sel.eesc.usp.br

Abstract - Recent advances in power generation technology and new directions in the Brazilian electricity regulation allowed wide spreading of the distributed generation (DG), with some consequent impacts on operational characteristics of the distribution networks. So, new methods for identifying such impacts become necessary in research and development of new tools and resources to maintain and ease the continued expansion towards DG deployment. Initially, this paper presents a study aiming at determination of the appropriate DG locations within distribution systems. This analysis presents a multicriteria analysis to define some qualitative and quantitative parameters using fuzzy logic to determine the appropriate DG sites. In this direction, the paper analyzes transient effects on the feeder power flow from which it is possible to determine the minimal conditions for guaranteeing DG reliability and high power quality. The considerations and results described in this paper make part of the Research & Development Program developed by the State Company for Electric Energy (CEEE) and the Federal University of Santa Maria (UFSM), Brazil.

***Keywords* – Appropriate DG sites, distributed systems, multicriteria analysis, power quality and transient effects.**

I. INTRODUCTION

Expansion of the distributed generation (DG) requires an appropriate modelling and analysis of the networks on which is going to be connected. Therefore, a general procedure for determining the appropriate DG sites becomes necessary so as to ensure that the DG effects on distribution systems are positive, and that they do minimize the electrical grid losses and maintain an acceptable voltage profile [1].

Manuscript received on April 22, 2008; revised on December 21, 2008 and April 01, 2009. Accepted by recommendation of the Editor Fernando L. M. Antunes.

A detailed evaluation of the feeder where the DG will be installed is also essential, as well as a good assessment of the supplied loads and their working states [2]. Without such assessments, the DG impacts on distribution networks may be more harmful than beneficial. The insertion of new generation sources in the distribution system may cause transient impacts due to switching operations and may change the existing levels of short-circuit and stability of the distribution system, causing erroneous operation of the protective devices [3] and likely islanding in parts of the system.

In Brazil, a set of laws and governmental programs encourage the development and installation of DGs by independent and self-producers [4-5]. However, there are different concepts among the electric energy companies because there are no agreements on the minimal conditions for connecting such sources, not even on what might happen on the DG protective system. Accordingly, the Brazilian National Regulatory Agency of Electric Energy (ANEEL) have implemented a project called Procedures for Distributing Electric Energy through the National Electric System (PRODIST) which aims at correct these deficiencies and many other omissions concerning the different issues related to planning and management of distribution systems. Section 3 of that document lists some of the minimal protective installations needed at a connection point with DG, together with actions that companies and producers must follow to guarantee quality and reliability in the production of electric energy [6].

Selection of optimal sites for DG is another important aspect mentioned in Section 3 of PRODIST. This paper therefore follows the PRODIST guidelines with respect to DG connection and location.

This paper analyzes both the quantitative and qualitative parameters to meet the appropriate DG sites. For example, parameters as voltage levels, cable loadings, power losses, the system average interruption frequency index (SAIFI), the system average interruption duration index (SAIDI) and number of clients supplied will be able to be quantitatively analyzed; on the other hand, access to a DG installation (considering presence of vegetation, for example), security (considering vandalism), physical space and ancillary services must be qualitatively considered. To cover these points, this paper presents a multicriteria analysis based on a membership fuzzy function and on the Bellman-Zadeh algorithm applied to a practical analysis to identify appropriate DG sites. It is important to emphasize that the methodology used to find the appropriate DG sites may be applied for distribution system feeders to find out which feeder is the most appropriate DG site, as well as to any node inside a given feeder to determine which node is the most appropriate for a DG location.

In addition to the steady state location of the DG, this paper presents an analysis in transient state of the impacts caused by DG when connected to the distribution system. This analysis will allow an evaluation of the minimal conditions suggested by ANEEL, satisfying all requirements concerning quality and reliability of the power supplied by the self-producers to the customers connected to the electric feeder.

II. BASIC CONSIDERATIONS OF DG PENETRATION

When an appropriate DG site is selected it must have a significant beneficial impact on power losses and an overall improvement of its voltage levels [7]. Recent technological advances are constantly providing new types of DERs (Distributed Energy Resources) for integrated SES (Storage Energy Systems) such as flywheels, batteries and ultra capacitors. These systems must be able to store energy for the subsequent electricity production, with a consequent improvement on the reliability and quality indexes. In terms of environment, some types of DER can reduce the greenhouse gas emissions, collaborating to preserve the global climate quality. Furthermore, DERs are not restricted to centralized high power generation, since the generating source can be placed closer to end-users. This also allows a structural rethinking of the electrical utility, diversifying and deploying the electrical energy sources to many generation sites, thus providing increased planning flexibilities. However, it is important to recognize that the power delivered by DER in inappropriate places, or an excess of power generation without voltage regulation, may result in increased system losses and undesired voltage levels that fail to satisfy the limits specified by national and international standards. This process may increase network costs and even impose penalties on the energy supplying companies. The DG connection may also introduce reversed power flows and interfere on the generating protection devices. For these reasons, a careful analysis of the DG connection consequences is extremely important, not only because the DG must satisfy certain geographical conditions, but also because they can degrade the reliability and quality of the power delivered to end-users.

III. MULTICRITERIA ANALYSIS

In this study a practical model was developed to validate the proposed methodology. This model is composed by a small substation feeder with 20 transformers (loads) connected to the grid (13.8kV/380/220, Δ – Y connection). Following the guidelines given by PRODIST-ANEEL, the two main sites for DG connection were selected from a previously-provided list of 5 candidate sites, taking into account the possibilities of these sites to support a DG location and concerning the energy supply company.

Regarding the multicriteria analysis [8-9], the methodology developed in this paper establishes the appropriate DG sites by using membership fuzzy functions based on quantitative criteria, a specific methodology used to analyze qualitative criteria and the Bellman-Zadeh algorithm to analyze outputs of these two methods altogether.

The parameters voltage levels (V_L), power losses and cable-loading (CL) were classified as quantitative criteria; whilst ancillary services, access, security and physical space were classified as qualitative criteria.

The quantitative criteria were analyzed considering two types of fuzzy functions. The power-loss criterion was analyzed using a trapezoidal function, defined by a set of equations, as shown in Figure 1. The main purpose of the DG connection in this case is to decrease power losses. Thus, sites where power losses are higher than 14% or lower than 2% have zero priority in the fuzzy function. Regarding the minimum limit, it is not necessary to reduce power losses in sites where these losses are already very low. In the case of the maximum limit, there will not be satisfactory the results during DG connection to sites with higher power losses because such sites will not be acceptable for other reasons and will require some improvement before DG is installed. However, DG connection will have a maximum priority where power losses are within acceptable levels, namely between 6% and 10%. In this case the DG connection may provide significant improvements on the network characteristics.

The voltage level criterion was analyzed using a modified form of the trapezoidal function defined by a set of equations as shown in Figure 2. The appropriate voltage levels (V_L) for energy delivery to customers are presented according to the rated level taken as its basis, in this case 220 V. This standard is established by ANEEL [10].

- Acceptable Voltage Levels (V): $201 \leq V_L \leq 231$;
- Warning Limits (V): $189 \leq V_L < 201$ or $231 < V_L \leq 233$;
- Critical Limits (V): $V_L < 189$ or $V_L > 233$.

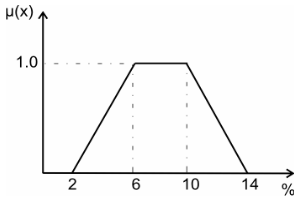

$$\mu(x) = \begin{cases} 0 & if\ x \leq 2 \quad or \quad if\ x > 14\% \\ 1 & if\ 6 < x \leq 10\% \\ 1 - \dfrac{(6-x)}{(6-2)} & if\ 2 < x \leq 6\% \\ \dfrac{(14-x)}{(14-10)} & if\ 10 < x \leq 14\% \end{cases}$$

Fig. 1. Trapezoidal function applied to the power-loss analysis defined by a suitable set of equations

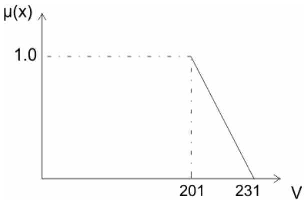

$$\mu(x)=\begin{cases}1 & if\ \ x<201\ V\\ \dfrac{(231-x)}{(231-201)} & if\ \ 201<x\leq 231\ V\\ 0 & if\ \ x>231\ V\end{cases}$$

Fig. 2. Trapezoidal function applied to voltage level analysis defined by its respective set of equations

The main objective of the DG installation in the analysis presented in Figure 2 is to improve the voltage profile. Thus, the maximum DG connection priority was attributed where there was a voltage profile below the minimum voltage level allowed by ANEEL. On the other hand, the minimum DG connection priority was attributed where the voltage levels are closer to the maximum limit allowed by ANEEL (231 V). In this case, the DG connection may provide a voltage level beyond the accepted limits.

To the cable-loading criterion (CL), it was assumed a linearly growing function, as shown in Figure 3. The maximum limit used in this case (75%) is related to the maximum current allowed through the cable. The main objective for using a DG connection in this analysis is to supply energy to loads and reduce the energy delivered by the substation so providing decreased current levels through all electrical cabling. Therefore, to determine where the DG connection has the highest priority, points must be identified where the cable is overloaded and consequently the current is higher than 75%. On the other hand, it was assumed that the priority decreases linearly where the currents are lower than 75%.

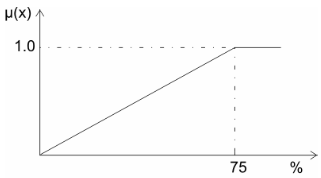

Fig. 3. Linear function applied to the cable-loading analysis

Regarding the qualitative criteria analysis, three specialists evaluated four criteria: ancillary services (X_1), security (X_2), access (X_3) and physical space (X_4). An average estimate is given by (1).

$$k_1=\frac{\sum\limits_{m} x_{ij}}{m} \tag{1}$$

where x_{ij} represents the comparison estimation between a pair of parameters, given by a specialist and m is the number of specialists. In (2) is given an example of analysis for the pair of parameters. This equation has been used as basis for this study.

$$\begin{aligned}X_i \succ X_j &\rightarrow x_{ij}=1.5; x_{ji}=0.5\\ X_i \approx X_j &\rightarrow x_{ij}=x_{ji}=1\end{aligned} \tag{2}$$

Since (2) gives values from each pair of parameters, an estimate k_2 is calculated by (3).

$$k_2=2-k_1 \tag{3}$$

The specialists (S1, S2 and S3) must therefore organize the parameters in its importance order, analyzing every criteria pairs. Table I is built to simplify the application of this method.

TABLE I
Arrangement of parameters regarding its importance

Pair of Parameters i,j	S1	S2	S3	k_1	k_2
X_1,X_2	1.5	1.5	1.0	1.33	0.67
X_1,X_3	1.5	1.0	1.5	1.33	0.67
X_1,X_4	1.5	1.0	1.5	1.33	0.67
X_2,X_3	1.0	0.5	1.5	1.00	1.00
X_2,X_4	0.5	0.5	1.5	0.84	1.16
X_3,X_4	0.5	1.0	0.5	0.67	1.33

In (4) is defined the priority coefficient of each parameter.

$$k_p=\frac{\sum\limits_{i=1}^{n} k_i}{n(n-1)} \tag{4}$$

where n is the number of parameters to be compared. In the next step, Table II is built to find results for k_p. In this window, the results for k_1 are positioned above the main diagonal of the matrix and the results for k_2 are positioned below it.

TABLE II
Coefficient of priority for each parameter

Parameters	X_1	X_2	X_3	X_4	Σ	k_p
X_1	-	1.33	1.33	1.33	4.00	0.333
X_2	0.67	-	1.00	0.84	2.50	0.208
X_3	0.67	0.67	-	0.67	2.00	0.166
X_4	1.00	1.16	1.33	-	3.50	0.292

In the next step, each specialist will attribute one weight (value from 1 to 10) for each parameter. Subsequently, the average estimate of parameters is calculated by adding these values divided by the numbers of specialists. Table III is built up by multiplying the average estimates by their respective k_p for each parameter. Thus, by adding these results it is possible to identify the maximum value. Later, the qualitative index (QAI) is calculated for each site, by dividing each summation by this maximum value. The QAI represents the final normalized values for the qualitative analysis. At the final step, a complete outcome is obtained according to quantitative and qualitative analyses and specialist estimates is obtained through the minimum operator method, represented by (5) and (6). This process results in a final index $Y(x)$ and a final ranking X^{th}, which shows the ranking of the appropriate DG sites, as presented in Table IV.

$$Y(x)=\arg min\mu(x) \tag{5}$$

$$X^{th}=\arg maxY(x) \tag{6}$$

TABLE III
Final normalized values for qualitative analysis

Sites	X_1	X_2	X_3	X_4	Σ	Priority QAI
	k_p= 0.333	k_p= 0.208	k_p= 0.166	k_p= 0.292		
G1	1.67	1.41	0.98	1.52	5.58	0.62
G2	1.83	1.29	1.20	2.01	6.33	0.70
G3	1.73	1.87	1.48	2.10	7.18	0.80
G4	2.63	1.73	1.18	2.25	7.78	0.86
G5	2.93	2.02	1.54	2.51	9.00	1.00

TABLE IV
Final DG placement ranking

Sites	Losses	CL	V_L	Priority QAI	$Y(X)$	X^{th}
G1	1.00	0.63	0.66	0.62	0.62	2nd
G2	0.76	0.55	0.78	0.70	0.55	5th
G3	1.00	0.79	0.61	0.80	0.61	3rd
G4	0.58	0.58	1.00	0.86	0.58	4th
G5	0.68	0.66	1.00	1.00	0.66	1st

Finally, it is possible to observe that sites G5 and G1 were the best sites for the DG installation, taking into account both quantitative and qualitative parameters.

IV. DISTRIBUTION SYSTEM MODEL: ANALYSIS IN STEADY-STATE OPERATION

Figure 4 presents the same distribution system model used in Section III. Now, this model is simulated in the software DigSilent® to evaluate the importance of the parameters voltage levels, power losses and cable-loading for the appropriate DG location. Furthermore, these simulations intend to compare the best and worst sites achieved in section III, represented by the nodes G5 and G2, respectively. The system in analysis is composed by a small substation feeder with 20 transformers (loads) connected to the grid (13.8kV/380/220, Δ–Y connection). Every load has a specific load curve, randomly connected along the main feeder path. To make the simulated system as realistic as possible, each line between nodes was dimensioned using standard cable dimensions.

As shown in Figure 4, a small generator unit was connected to each node G1, G2, G3, G4 and G5. Node G5 is located at 83.5 km from substation (SS) and node G2 at 29.5 km from SS. These DERs supply specific power generation, representing about 14% of the whole electrical load at the peak hour. These units operate only between the 18h and 21h, since within this period it is included the peak hour. When the generator is supplying 150 kVA to node G5, positive impacts on the operational characteristics of the distribution system were observed, such as voltage levels improvement at node G5 and power losses (PL) and current levels (I_L) decrease in the whole grid, as shown in Table V.

When the generator supplies 150 kVA to node G2, a considerable increase in the voltage profile of this node and decreased power losses and current levels through the whole grid are observed, as shown in Table VI. In this case, the period between the 21h and 22h (21h in Table VI) must be noted because the lowest demand for DG operation occurs within this period, and, consequently, the highest voltage level. In that period, the voltage level reaches 228.9 V, closer to the maximum level allowed by ANEEL (231 V). It is therefore necessary to verify the entire period during the DG operation. In this way, an exceeded voltage profile can be avoided.

TABLE V
Voltage levels at node G5 and power losses and current levels in the whole grid with DG connection

Time	Without DG	With DG	With DG	With DG	With DG
(h)	V_L (V)	V_L (V)	ΔV_L (%)	ΔI_L (%)	ΔPL(%)
18	204.0	223.6	+ 9.61	- 30.35	- 66.60
19	198.6	219.1	+10.32	- 26.58	- 60.48
20	202.3	222.1	+ 9.79	- 28.81	- 63.97
21	205.9	225.1	+ 9.32	- 32.17	- 68.86

TABLE VI
Voltage levels at node G2 and power losses and current levels in the whole grid with DG connection

Time	Without DG	With DG	With DG	With DG	With DG
(h)	V_L (V)	V_L (V)	ΔV_L (%)	ΔI_L (%)	ΔPL(%)
18	217.8	226.9	+ 4.18	- 21.74	- 30.40
19	215.4	224.7	+ 4.32	- 18.20	- 26.29
20	216.9	226.1	+ 4.24	- 20.38	- 28.65
21	218.6	228.9	+ 4.12	- 23.27	- 31.71

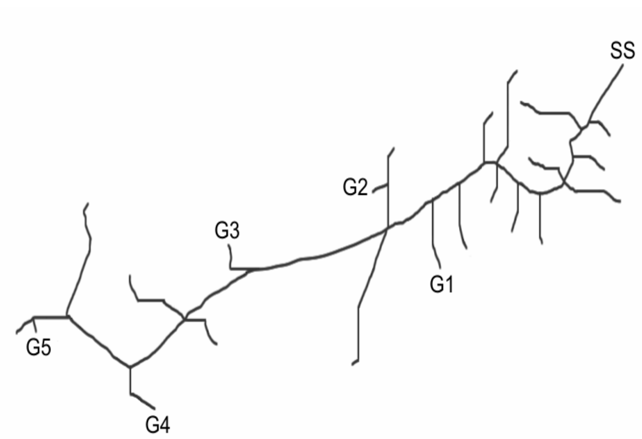

Fig. 4. Distribution system model with an interconnected DG as basis for this study, simulated in the software DigSilent®

V. DG SYSTEM: ANALYSIS OF TRANSIENT STATE OPERATION

Another important issue is the effects that a DG system may cause on the distribution system when it is connected to a feeder. A power plant connected to node G1 represents a secondary source and the feeder used as standard for this study is a specific distribution system.

Node G2, in Figure 5, represents an extra source; however, it was not used in the transient analysis. To connect the DG to the feeder, a set of high power converters was used. For both converters, a frequency of 12 kHz was used as the PWM switching frequency [11]. To avoid disturbances between the DC-AC converter and the feeder, a phase locked-loop (PLL) algorithm associated to voltage zero crossing detectors has been used.

A. Power system analysis

A single-line equivalent diagram of the power system, as shown in Figure 4 and expanded in Figure 5, was used to investigate the typical scenario when connecting a distributed generation system to a specific feeder. In this case, previous studies about the best site for a DG connection were taken into account (as presented in section III of this paper). The system is made of 13.8 kV feeders connected to a large network through a 69 kV radial line. The 13.8 kV substation busbar is connected to the main grid through the substation transformer. The grid is represented according to the short-circuit capacity, so that, the high short-circuit power, the less susceptible the system become to rapid disturbances. It means higher short-circuit power, so lower equivalent impedance values were obtained. The grid parameters are defined by (7) and (8).

The line model is based on the Bergeron's traveling wave method used in Electromagnetic Transient Program (EMTP). This model can represent the wave propagation phenomena and the line end reflections.

The DG system is connected to node G1. In this way, to connect the AC converter into the feeder an $L_{conv}.C_{conv}.L_S$ filter was used. The distribution transformer is also used to match the distribution voltage levels and, a solid state relay is inserted to isolate the DGs when any contingence is observed on the high voltage side of the distribution transformer.

$$L_{grid} = \frac{V_{AB}^2}{8\pi P_{SC} f} \tag{7}$$

$$R_{grid} = \frac{(2\pi f) L_{grid}}{X}, \; 1 < X < 100 \tag{8}$$

B. Energy control in the feeder

Power balance means sinusoidal, symmetric and balanced voltages on the AC bus side to control the energy produced by the DC sources. A coupling inductor (L_S) is used to connect the DG to the feeder and it does not represent any of the grid parameters. DG then provides reactive power and harmonic compensation without any kind of current distortion measurement to the load, which ensures that the feeder delivers and/or absorbs only active power. In fact, the filtering effectiveness of the system depends on the inverter output impedance compared to other system impedances (load and feeder) [12].

In order to control the power flow, it is necessary to adjust the local AC bus voltage amplitude (V_A), the β angle between phasors $\boldsymbol{V_A}$ and the feeder phase voltage ($\boldsymbol{V_{source}}$). If phasors $\boldsymbol{I_{source}}$ (feeder current) and $\boldsymbol{V_{source}}$ have the same direction, the system will deliver power to the feeder. When they have opposite directions the system consumes power, Figure 6 [13-14].

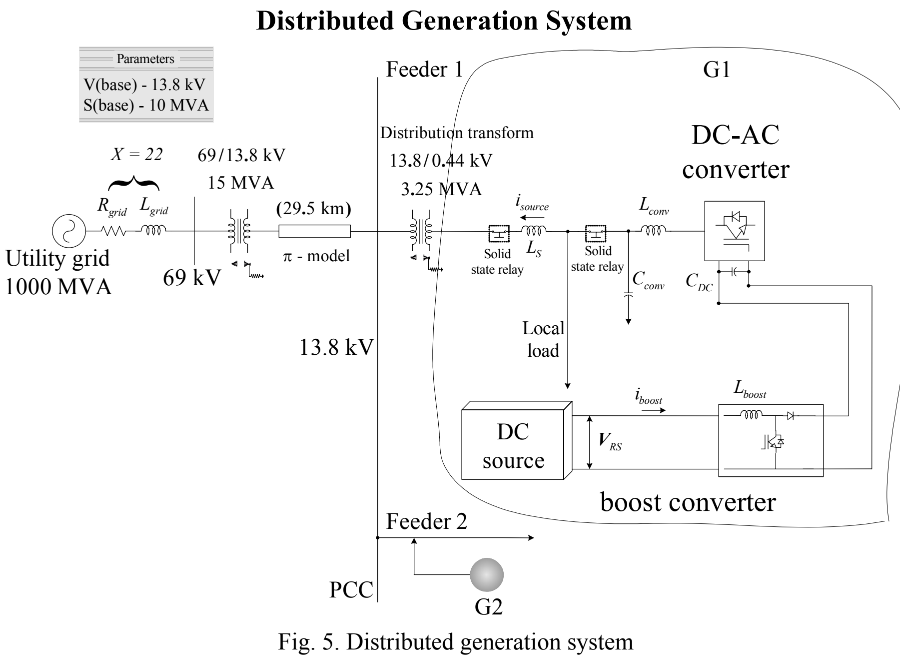

Fig. 5. Distributed generation system

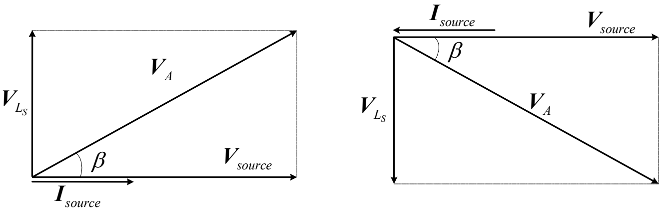

(a) Absorbing power (b) Delivering power

Fig. 6. Phasor diagrams

To determine the β angle one have to know the difference between generated and locally consumed single-phase power ($P_{source}/3$), to access the connecting reactance (X_{L_S}) and measure the rms feeder phase voltage according to (9).

$$\beta = \arctan\left(\frac{P_{source} X_{L_S}}{3V_{source}^2}\right) \quad (9)$$

After defining the β angle, it is necessary to adjust the voltage amplitude V_A according to (10) assuring a unity power factor in the feeder. With regard to the amplitude V_A, a minimal variation is expected because both Brazilian and international standards do not allow any specified limits to be exceeded. For that, the coupling inductor [13-14] is designed for small voltage variations on the AC local voltage produced by the DC-AC inverter. Additional information about (9) and (10) is explained in details in Appendix.

$$V_A = \frac{V_{source}}{\cos\beta} \quad (10)$$

C. DC-DC converter

A DC-DC step-up converter was used as the interface between the DC source and DC bus of the DC-AC converter. Its main objective is not only to boost the DC voltage but also to supply the fast transient energy required for the local load, avoiding disturbances on the feeder current. In this way, a load connection alters the AC voltage from the AC converter and consequently the DC voltages are regulated by the boost converter. As a cascade control (Figure 7) is employed, the output of the DC voltage controller (current reference) is changed to compensate the error in voltage across the DC bus. Hence, the step-up converter behavior is quite similar to a voltage source and its power delivered to the feeder depends on the point of maximum power (PMP) defined by the DC source.

The PMP is obtained by a tracking algorithm dependent on the maximum solar incidence (PV panel) or the injection of fuel (fuel cell), according the type of primary energy source. During fast transients (load connection), an ultra capacitor could supply the extra energy required by the local load. Furthermore, an isolated step-up converter could also be used to improve system stability. Hence, PIs controllers were used as the control technique to stabilize the current through $L_{boost} = 5$ mH and the DC voltage, as shown in Figure 7.

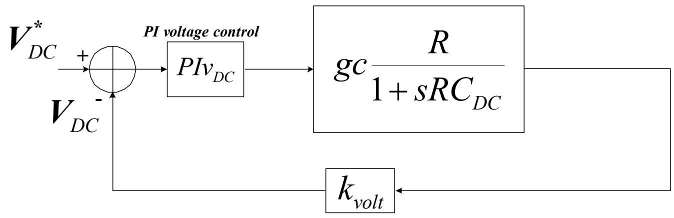

Fig. 7. Block diagram of the boost

A method based on phase-margin ($mf = 80^o$) and cut-off frequency ($\omega_{FCL} = 2500$ rad/s) was used to obtain the PI constants (11) and (12) where the open loop gain (G_{OL}), ω_{FCL} and mf define the PI constants (k_{prop} and k_{int}). The constant k_{volt} is the voltage gain, R is the rated load, and gc is the transfer function to represent the current control of the boost converter.

$$k_{prop}\frac{G_{OL}}{\omega_{FCL}} = 1 \quad (11)$$

$$k_{int} = k_{prop}\frac{\omega_{FCL}}{tan(mf)} \quad (12)$$

D. DC-AC converter

Closed loop controls of the output current and voltage were implemented to assure inverter voltage quality. PI controllers were also selected as control technique and design method of these PIs since they are the same ones used in the DC-DC step-up converter.

As closed loop cut-off frequency of the current PI was selected as one decade below the switching frequency, the current PI has still a good compensation capability within the frequency range of interest. To improve this capability, a feed-forward reference voltage could be used to compensate residual errors in the closed loop gain at low frequencies [12-13].

Due to the high power and the need for a reduced switching frequency, the voltage controller exhibits low regulation bandwidth (a few hundred Hertz). To cope with that and to provide good output voltage control for both fundamental and harmonic components, a selective filter was placed in parallel across the conventional voltage regulator so reducing the converter impedance. Details about the control scheme and the main parameters used to design both AC PIs can be found in references [12-13].

E. Synchronization algorithm

Representing the PLL structure corresponds to an internal product of two orthogonal signals [15-16].

$$H_{CL} = \frac{k_p s + k_i}{s^2 + k_p s + k_i} \quad (13)$$

In this way, a canonical form of a second-order system can adjust the PI constants (14) and (15). To avoid stability problems is common practice to use ω_n larger than 1 or 2 periods of the fundamental frequency, in this case 60 Hz.

$$k_p = 2\xi\omega_n \qquad (14)$$

$$k_i = \omega_n^2 \qquad (15)$$

VI. SIMULATIONS: TRANSIENT ANALYSIS

This section presents the simulations performed with the MatLab® software.

A. Connection and transference of power

Two procedures are employed to connect the DG system to the feeder. As a first step, it was used an algorithm to synchronize v_{source} and v (voltage produced by the DC-AC converter). After synchronization, the voltage zero crossing algorithm of v_{source} is initiated. After terminating the zero crossing algorithmes, the relay connecting both systems is closed, so minimizing feeder transients. At last, the power transfer can be initialized. A soft transfer operation mode (80 kVA/s) followed by a base load operation is used to test this capability. Due to the method employed - synchronization and soft transference of power - there are not noticeable disturbances across the feeder, as shown in Figure 8.

B. Load transient

In this test, a 40 kVA/s power transference was carried out. After the soft power transfer, two sets of linear loads were connected across within a short interval of time. In this case, the energy storage is quickly transferred to local load so minimizing energy transients through the feeder. Fraction of power needed for load supply after stabilization is supplied by the feeder, since the maximum power produced by the DG system itself is not able to supply such a load (Figure 9). Figure 10 depicts all these variables after system stabilization. It is possible to observe that $\boldsymbol{v}_{source}$ and $\boldsymbol{i}_{source}$ have opposite directions.

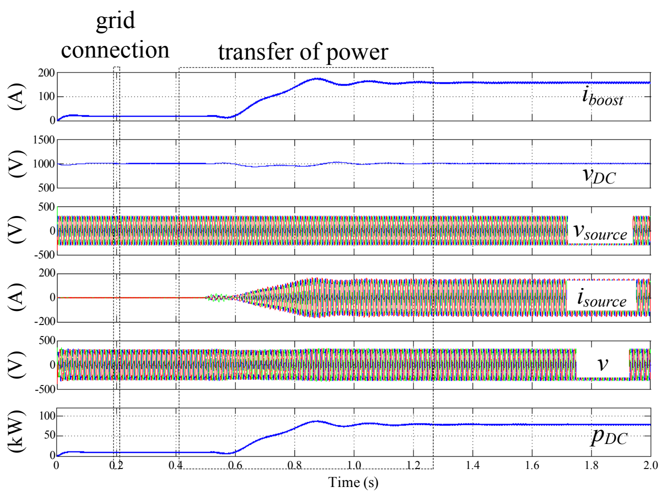

Fig. 8. Connection of DG system to a feeder

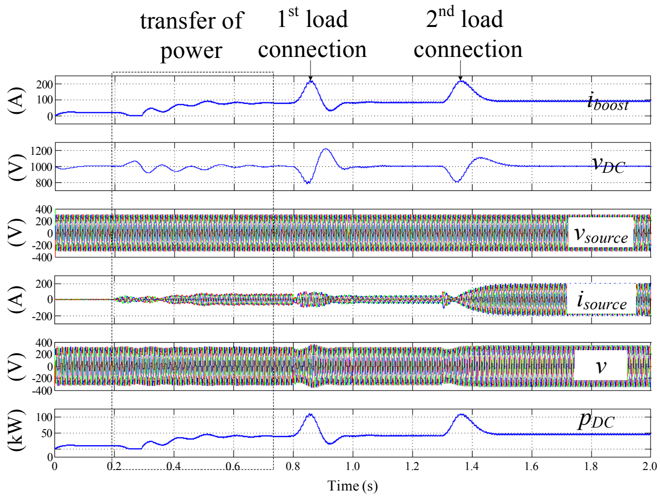

Fig. 9. Load transient

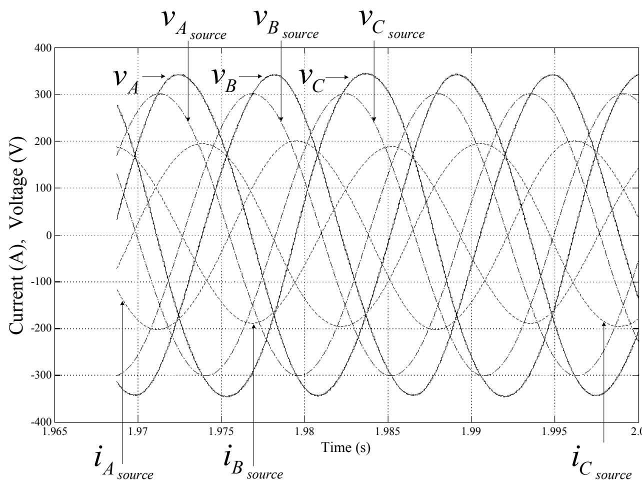

Fig. 10. Steady state analysis with high power linear load

C. Islanding mode considerations

The island mode can be caused by short-circuits followed by protecting device actions on the high voltage side of distribution transformers connecting DG system and feeder. When it occurs, the islanding mode is detected and its management is undertaken by the islanding algorithm causing an abnormal system operation. Following this idea, when a minimal level of active power is transferred to the feeder, the effect caused by the islanding on the power through the distribution transformer or the DC bus voltage is minimal in comparison to load connection or power transfer, Figure 11.

D. Islanding and reconnection to the feeder

The capability of the studied DG system to absorb high disturbances is evident when an islanding is followed by reconnection procedures. In this case, when an islanding occurs, the switch connecting the DG to the feeder is rapidly opened, so that DG does not supply loads connected across the high voltage side of the distribution transformer. This fact could cause a DG collapse if these loads demand for more power than that produced by the DG system. After re-connection of the feeders, the synchronization must start on and the DG switch now can be closed. When the feeder is reconnected again, the local load represents a low impedance path for the feeder. Thus, it supplies almost instantly the local load, as shown in Figure 12.

VII. CONCLUSION

This paper discusses a general multicriteria fuzzy method in which some membership fuzzy functions and the Bellman-Zadeh algorithm were used to find out the most appropriate DG location, concerning both quantitative and qualitative parameters.

The first part of this paper describes the analysis of quantitative parameters such as power losses, voltage levels and cable-loading by using a distribution system model simulated in the software DigSilent®. The second part of this paper was simulated in the software MatLab®. It shows that connection of DG sources driven by parallel DC-DC and DC-AC converters across the feeder may cause impacts if connection procedures are properly not taken into account. These procedures should not only be able of synchronizing the DG system and feeder, but also to find out the best connection instant for both systems that is, at zero crossing of the source voltage. Fast load transients across the feeder are not observed because the boost converter controls the DC voltage. However, the DC-DC converter must be able to deliver rapidly this additional energy. In this case, an ultra capacitor might be employed. Finally, taking into account the constant DG wide spreading in electric power systems and their significant impacts on the operational characteristics of distribution networks, it is essential to develop careful analyses of consequences of a DG connection, evaluating the most appropriate DG locations and contributing so for the distribution system planning.

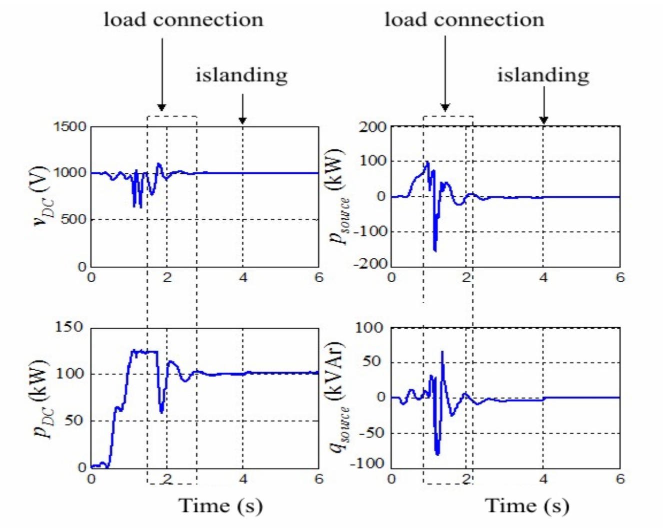

Fig. 11. Islanding for zero power flow

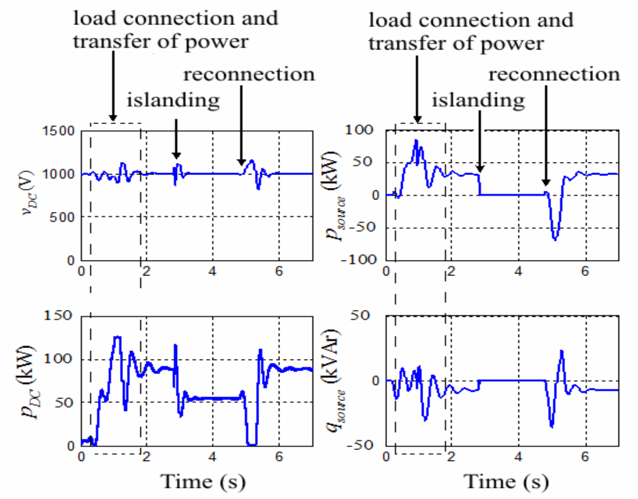

Fig. 12. Islanding and reconnection effects on power flow

ACKNOWLEDGMENT

The authors would like to thank CAPES for their financial support.

APPENDIX

As L_s is designed to obtain small angle β (from the no power to the rated power mode) and due to non-circulation of the reactive power required for the system ($Q_{source} \cong 0$), it is possible to establish the system behavior as proposed in this paper according the diagram presented in Figure 6. In this case, (9) it is obtained by rearranging (16) and (17). In (9) $P_{source}/3$ represents the single-phase power flow calculation.

$$\tan\beta = \frac{\sin\beta}{\cos\beta},\ \sin\beta = \frac{V_{L_S}}{V_A} \text{ and } \cos\beta = \frac{V_{source}}{V_A} \tag{16}$$

$$\frac{P_{source}}{3} = \frac{V_{source_{rms}} V_{A_{rms}}}{\left|X_{L_S}\right|}\sin\beta \tag{17}$$

According to (10), the assumption of a no reactive power is sufficient to set $Q_{source} \cong 0$ (single-phase power) in (18).

$$Q_{source} = \frac{V^2_{source_{rms}}}{\left|X_{L_S}\right|} - \frac{V_{source_{rms}} V_{A_{rms}}}{\left|X_{L_S}\right|}\cos\beta \tag{18}$$

To obtain a high power factor at the point of common coupling (PCC) i_{load_A}, i_{load_C}, i_A, i_C, v_A, v_C and $v_{A_{source}}$ are measured. The residual power (P_{source}) to be transferred to or absorbed from the feeder are then calculated by (19) and (20), where P_{DC} represents the power produced by the DG system.

The angle β and amplitude V_A are respectively calculated by (9) and (10). The references (v_B and v_C) are shifted by 120º and -120º with respect to v_A whereas the synchronism between the inverter AC voltage and the feeder voltage is achieved by using a PLL algorithm as presented in Section V.

$$P_{load} = \frac{1}{T}\int_0^T \left(i_{load_A} v_A + i_{load_B} v_B + i_{load_C} v_C \right) dt \qquad (19)$$

$$P_{source} = P_{DC} - P_{load} \qquad (20)$$

REFERENCES

[1] A.Barin, L.F. Pozatti, L. N. Canha, F.A. Farret, R.Q. Machado, A. R. Abaide, C. Carvalho, C.E.M. Fernandes, "Analysis of the Impact of Distributed Generation Sources on the Operational Characteristics of the Distribution Systems for Planning Studies", *in Proc. of 19th International Conference on Electricity Distribution,* 2007.

[2] C. L. T Borges, D.M. Falcão, "Impact of distributed generation: Allocation and sizing on reliability, losses and voltage profile", *in Proc. of IEEE Power Tec. Conference, Italy*, 2003.

[3] S. Chaitusaney, A. Yokoyama, "Impact of Protection Coordination on Sizes of Several Distributed Generation Sources", *in Proc. of 7th International Power Engineering Conference*, 2005.

[4] Brazilian Law n° 2003, September 1996.

[5] Brazilian Law n° 10438, April 2002.

[6] National Regulatory Agency of Electrical Energy - PRODIST (Section 3), Brazil, 2008.

[7] J. Choi, J. Kim, "Network Reconfiguration at the Power Distribution System with Dispersed Generations for Loss Reduction", *in Proc. of Power Engineering Society Winter Meeting*, vol. 4, pp. 363-367, 2000.

[8] P. Ekel, L. D. B. Terra, M. F. D. Junges, "Methods of multicriteria decision making in fuzzy environments and their applications to transmission and distribution problems", *Fuzzy Information Processing Society, IEEE, in Proc. of 18th International Conference of the North American, 1999*.

[9] L. N. Canha, *Metodologia para localização e dimensionamento de pequenas fontes de geração distribuída em redes de distribuição a partir de uma análise multicriterial*, Doctorate thesis, Federal University of Santa Maria, pp. 313, 2004.

[10] National Regulatory Agency of Electrical Energy - ANEEL, Resolution 505, November 26th, Brazil, 2001.

[11] http://www.siemens.com, last access: May 2007.

[12] P. Mattavelli, "A closed-loop selective harmonic compensation for active filters", *IEEE Transactions on Industry Applications*, vol. 37, issue 1, pp. 81 –89, 2001.

[13] R. Q. Machado, S. Buso, J. A. Pomilio, "A Line-interactive Single-phase to Three-phase System", *IEEE Transactions on Power Electronics*, vol. 21, issue 6, pp. 1628 – 1636, 2006.

[14] R. Q. Machado, S. Buso, J. A. Pomilio, "Grid Interaction of a Single-phase Feeder to a Three-phase Converter", *Eletrônica de Potência - Sobraep*, vol. 13, issue 4, pp. 185 – 192, 2008.

[15] F. P. Marafão, S. M. Deckmann, J. A. Pomilio, R. Q. Machado, "Metodologia de Projeto e Análise de Algoritmos de Sincronismo PLL", *Eletrônica de Potência - Sobraep*, vol. 10, issue 1, pp. 07 – 14, 2005.

[16] V.Kaura,V.Blasko,"Operation of a Phase Locked Loop System under Distorted Utility Conditions", *IEEE Trans. on Industry Application*, vol. 33, issue 1, pp. 58 – 63, 1997.

BIOGRAPHIES

Alexandre Barin was born in Santa Maria, Brazil. He received the Bachelor's degree from the Federal University of Santa Maria in 2005 and the Master's (2007). Currently he is a doctorate student in Electrical Engineering of the Federal University of Santa Maria. He is a Student Member of IEEE since 2006.

Luis Felipe Pozzatti was born in Santa Maria, Brazil. He received the Bachelor's degree from the Federal University of Santa Maria in 2004. Currently he is working at Eletrosul S.A.

Ricardo Quadros Machado was born in Santa Maria, Brazil. He received the Bachelor's degree from the Federal University of Santa Maria in 1997, Master (2000) and Ph.D. (2005) degrees in Electrical Engineering also from the Federal University of Campinas, Brazil. From 2002 to 2003 he worked as visiting researcher at the University of Padova, Italy, and from 2005 to 2007 he followed a post-doctoral program at the Federal University of Santa Maria in alternative sources of energy. Nowadays, he teaches in the Department of Electrical Engineering at the University of São Paulo/São Carlos. Dr. Machado is a full member of IEEE and SOBRAEP.

Luciane Neves Canha was born in Santa Maria, Brazil. She received the Bachelor's degree from the Federal University of Santa Maria in 1994, Master (1996) and Post-Graduated as Doctor in Electric Engineering (2004). She has been professor and researcher at the Federal University of Santa Maria since 1997.

Felix A. Farret was born in Santa Maria and received his B.E. and M.Sc. in electrical engineering from the Federal University of Santa Maria in 1972 and 1986, respectively. He also received certification as a specialist in instrumentation and automation from the Osaka Prefectural Industrial Research Institute, Japan; M.Sc. from the University of Manchester, England, in 1981 and Ph.D. from the University of London, Imperial College, England, in 1984, all in electrical engineering; and completed the Post-Doctoral Program in Alternative Sources of Energy at the Colorado School of Mines in 2003. He was a visiting professor at Colorado School of Mines, Engineering Division, from 2002 to 2003. He published his first book in Portuguese, Use of Small Sources of Electrical Energy (UFSM University Press, 1999), co-authored the book Renewable Energy Systems: Design and Analysis with Induction Generators (CRC Press, second edition, 2008) and authored the book Integration of Alternative Sources of Energy (John Wiley & Sons, 2006). He has been professor and researcher at the Federal University of Santa Maria since 1974.

Alzenira da Rosa Abaide was born in Santa Maria, Brazil. She received the Bachelor's degree from the University of Santa Maria in 1957, Master's (2000) and Post-Graduated as Doctor in Electric Engineering (2005). She worked as engineer from 1986 to 1988 in State Company of Electric Energy. She has been professor and researcher at Federal University of Santa Maria since 1989.